

## Isothermal acid-titration calorimetry for evaluating the pH dependence of protein stability

Shigeyoshi Nakamura<sup>a</sup>, Shun-ichi Kidokoro<sup>a,b,c,\*</sup>

<sup>a</sup>*Department of Bioengineering, Nagaoka University of Technology, 1603-1 Kamitomioka, Nagaoka 940-2188, Japan*

<sup>b</sup>*Precision and Intelligence Laboratory, Tokyo Institute of Technology, 4259 Nagatsuta, Midori-Ku, Yokohama 226-8501, Japan*

<sup>c</sup>*Genome Science Center, Riken, 1-7-22 Suehiro-cho, Tsurumi-ku, Yokohama 230-0045, Japan*

Received 2 October 2003; received in revised form 19 November 2003; accepted 20 November 2003

### Abstract

A new method, which can be called as isothermal acid-titration calorimetry (IATC), was proposed for evaluating the enthalpy of protein molecules as a function of pH using isothermal titration calorimetry (ITC). This measurement was used to analyze the acid-denaturation of bovine ribonuclease A. The enthalpy change by acid-denaturation of this protein was estimated as 310 kJ/mol at pH 2.8 and 40 °C. This value agreed well with the enthalpy change obtained by differential scanning calorimetry. The midpoint pH and proton binding-number difference observed by IATC agreed well with those of the acid transition of the three-dimensional structure monitored by circular dichroism spectrometry. The van't Hoff enthalpy of the transition was derived from the temperature dependence of the midpoint pH and the proton binding-number difference. It agreed well with the calorimetric enthalpy change directly observed by IATC, strongly indicating that there was no stable intermediate state during the acid transition of this protein. © 2003 Elsevier B.V. All rights reserved.

**Keywords:** pH Dependence; Enthalpy; Acid transition; Ribonuclease A; Two-state transition; Heat capacity change

### 1. Introduction

The protein three-dimensional (3D) structure is realized as the most stable thermodynamic state, which is a necessary condition for the automatic folding of the protein molecule. Accordingly, obtaining a more complete thermodynamic understanding of the folding mechanism has become one of the most important and interesting challenges in the field of protein physics.

Our thermodynamic knowledge of protein thermodynamic stability has been considerably improved over the last several decades by calorimetry, a direct method to measure the thermodynamic functions [1–13]. In particular, adiabatic differential scanning calorimetry (DSC) has enabled us to determine the enthalpy of a protein molecule precisely as a function of temperature, and the Gibbs free energy can be evaluated from the enthalpy using a thermodynamic relationship [14–16]. The thermodynamic changes accompanying the phase transition of the protein 3D structure, such as the Gibbs free energy change, the

\*Corresponding author. Tel./fax: +81-258-47-9425.

E-mail address: kidokoro@nagaokaut.ac.jp  
(S.-i. Kidokoro).

enthalpy change, and the entropy change, are easily evaluated from the calorimetry data.

In principle, even the second temperature-derivative of the Gibbs free energy change, the heat capacity change, can be evaluated by observing the difference between the heat capacities of the native and the heat-denatured state, directly with DSC. In the present study, we denote the heat capacity change evaluated by this direct method as the ‘calorimetric heat capacity change’ or ‘directly observed heat capacity change’ under constant pH. The heat capacity change is considered to be mainly the result of the change of the hydration of the protein molecule accompanying the structural transition, and is important for understanding the mechanism of protein stability [17–19].

In practice, however, the heat capacity change has been estimated from the slope of the  $\Delta H(T_m)$  vs.  $T_m$  plot, where  $T_m$  is the midpoint temperature of the thermal transition and  $\Delta H(T_m)$  is the enthalpy change at the temperatures evaluated under several pH conditions [2,20]. While the ‘calorimetric heat capacity change’ can be determined under a single pH condition but with a fairly large experimental error, the linearity of the  $\Delta H(T_m)$  vs.  $T_m$  plot, which can be observed in many cases, is convenient to determine the slope precisely over a wide range of  $T_m$  values—namely, over a wide pH range. In the case of non-calorimetric measurement, such as spectroscopic measurement, the heat capacity change can be estimated only by using this plot.

In theory, however, the slope deviates from the real heat capacity change if the enthalpy change has pH dependence; this can be easily shown as follows [21]. The  $T_m$  dependence of the enthalpy change at the midpoint temperature,  $\Delta H(T_m)$ , is described as:

$$\frac{d\Delta H(T_m, \text{pH})}{dT_m} = \Delta C_p(T_m, \text{pH}) + \left. \frac{\partial \Delta H}{\partial \text{pH}} \left( \frac{dT_m}{d\text{pH}} \right)^{-1} \right|_{T_m, \text{pH}} \quad (1)$$

where  $\Delta C_p$  is the heat capacity change. In the

second term of the right-hand side of Eq. (1), the pH dependence of the midpoint temperature is determined experimentally by DSC, while the pH dependence of the enthalpy change under constant temperature cannot be evaluated without knowing the heat capacity change by DSC. Because the enthalpy of the native state has been reported to show a clear pH dependence due to the protonation/deprotonation enthalpy [22,23], and the  $pK_a$  values of the protein residues in the denatured state are not identical to those in the native state, the enthalpy change cannot be expected to be independent of pH. If the pH dependence of the enthalpy change is large, the slope systematically deviates from the heat capacity change. Indeed, some papers have reported that calorimetrically observed heat capacity changes deviated remarkably from the slope [24–26]. In other reports, however, these values agreed with the slope [2]. Therefore, it is important to determine the contribution of the pH dependence of the enthalpy change to the slope in order to evaluate the heat capacity change accurately.

Calorimetry is a powerful method for measuring the pH dependence of enthalpy. To our knowledge, however, there have been few reports on the enthalpy change of protein molecules induced by pH change. Initially, flow calorimetry was used to measure the enthalpy of acid denaturation of lysozyme [22]. The high protein concentration and the large amount of protein necessary for the measurement, however, have prevented this method from becoming a general tool for evaluating the pH dependence of protein stability. In a subsequent study, titration calorimetry was applied to observe the acid denaturation of a small globular protein, the B-subunit of cholera toxin, but the observed transition did not agree with the observed transition by DSC, which was estimated to be a partial unfolding [27]. Titration calorimetry was also applied to observe the structural change of cytochrome *c* from the acid-denatured state to the molten globule (MG) state by titrating salt to stabilize the MG state [28]. The enthalpy change of the folding reaction determined by this method agreed with that determined by the DSC method, and the power of titration calorimetry for evaluating the protein stability was shown clearly, since

the concentration and amount of protein required were almost comparable to those for DSC. However, the salt-titration folding/unfolding was not generally applicable in characterizing the structural change from the native state, and the high salt concentration necessary for protein folding/unfolding led to a severe problem in terms of the required correction for the dilution heat of salt-titration. Recently, an attempt was made to use acid-titration calorimetry to monitor the acid-denaturation of the MG state of apomyoglobin [23]. The authors concluded that the enthalpy change of this transition was too small to be observed, and thus that there was no thermal transition, a conclusion compatible with the DSC findings. Although acid-denaturation was not observed in this article, the dilution heat by acid-titration was not very large, and could be corrected to determine the enthalpy as a function of pH by acid-titration calorimetry. Because protons are the general ligands for all kinds of protein molecules, and protein stability depends largely on the pH of the solution, we considered that acid-titration calorimetry has great potential as a general tool to measure protein stability. To the best of our knowledge, however, there has been no clear and quantitative observation of the pH transition of protein molecules using isothermal titration calorimetry.

In this article, we propose an isothermal acid-titration calorimetric (IATC) technique that incorporates several new methods and that can be used to obtain the precise enthalpy function of pH, such as evaluation for acid-dilution heat with several injection volumes, joint method with different acid concentration, and data analysis with appropriate pH functions for the enthalpies of native and acid-denatured states and for the change of proton binding-number between these states. As the van't Hoff enthalpy is calculated by analyzing the temperature dependence of the stability, we also proposed an equation for evaluating the enthalpy from IATC.

In order to test their efficacy, these techniques were used to observe a two-state acid-denaturation of bovine ribonuclease A. The structural transition was also directly observed by far ultraviolet circular dichroism spectrometry, and the results were compared to those by IATC. DSC evaluation of

the enthalpy change accompanying the thermal denaturation of the protein was also compared to that of IATC. Finally, the pH dependence of the enthalpy change of this protein was evaluated, and an attempt was made to determine the heat capacity change of acid-denaturation using only IATC analysis.

## 2. Materials and methods

### 2.1. Preparation of ribonuclease A for acid-titration calorimetry

Lyophilized powder of bovine ribonuclease A (R-5500; Sigma, St. Louis, MO, USA) was dissolved as 0.5 mg/ml solution with 20 mM NaCl. This protein solution was dialyzed with a dialysis membrane, Spectra/Por (132660; Spectrum Lab., Rancho Dominguez, CA, USA) whose cut off molecular weight was 6000–8000 at 4 °C for 4–10 days against 2L 20 mM NaCl solution with several changes of the solution. Before the acid titration, 50 mM NaOH (Wako, Osaka, Japan) was added to the protein solution in order to adjust the pH to 6.5–7.5. The pH measurement was performed with a glass electrode and F14 pH meter (Horiba, Kyoto, Japan). The reading of pH values was corrected using the standard pH solutions for pH 2, 4 and 7 (Horiba, Kyoto, Japan) at the temperature for the measurement. The concentration of bovine ribonuclease A was determined spectrophotometrically with a spectrophotometer, UB-35 (Jasco, Tokyo, Japan) by using an extinction coefficient  $A_{278}^{1\%} = 7.1 \text{ OD cm}^{-1}$ . If the apparent absorbance at 350 nm was larger than 0.01 OD cm<sup>-1</sup>, the protein solution was ultra-filtrated with a MolCut ultra filter unit (USY-20; Advantec, Tokyo, Japan) whose cut off molecular weight was 200 kDa in order to remove the aggregate being produced during the dialysis, and the absorbance spectrum of the filtered protein solution was re-evaluated. The degassing of the solution was performed completely for several minutes by aspiration with a ULVAC membrane pump (Sinku Kiko, Kanagara, Japan) and simultaneously sonicated with a small sonication, Perl Clean (Fkk, Tokyo, Japan). The 50, 100, 200 and 500 mM HCl solution with 20 mM NaCl was made by

dilution of 1 M HCl (Nacalai Tesque, Kyoto, Japan).

## 2.2. Acid titration calorimetry

The HCl-titration to ribonuclease A was performed using an isothermal titration calorimetry unit of MCS (MicroCal, Northampton, MA, USA) at several temperatures ranging from 15 to 65 °C. The protein solution was loaded in the ITC sample cell, the volume of which was 1.3684 ml. Titration was done with injections of 0.5–15  $\mu$ l each of 50–500 mM HCl solution in 20 mM NaCl using a 250  $\mu$ l syringe. Before each experiment, the ITC cell was washed several times with a blank solution of 20 mM NaCl. The control experiment was performed with the absence of protein solution throughout the same pH range.

The heat absorption,  $\Delta Q$ , during and after each injection was calculated by time-integration of the compensation power,  $dQ/dt$ , directly observed as the function of time by ITC, from which the calculated baseline was already subtracted. These calculations were processed by a program, Origin, supplied by the manufacturer of the calorimeter.

The observed heat was expressed as a function of pH by monitoring the pH of the titrated protein solution as described below, and subtracting the dilution heat of HCl at the same pH of the protein solution as described in Section 2 to determine the dilution heat. The enthalpy of the protein molecule was calculated by summing the corrected heat effect after each injection.

The calorimeter was calibrated by monitoring the neutralization heat of NaOH and HCl. The 1.0  $\mu$ l of 50 mM HCl was titrated to 50 mM NaOH with a 100  $\mu$ l syringe at 25 °C. In the calibration process, three different control titrations were also performed—i.e. water was titrated to NaOH, HCl was titrated to water, and water was titrated to water. Although all of the observed heat values in these control titrations were much smaller than those in the neutralization titration, the heat of neutralization was corrected by using the heat values of control titrations. The heat of neutralization, 55.7 kJ/mol at 25 °C [29], was used to calibrate the calorimeter.

## 2.3. The pH measurement of acid titration

The pH measurement of HCl-titration to ribonuclease A was performed using a glass electrode and pH meter, F14 (Horiba, Kyoto, Japan), at the same temperatures as IATC measurement. The solutions measured by the pH meter were identical to those used in IATC. In the pH measurement, the initial volume of the protein solution was 10 ml, and the injection volumes were determined, as the ratio between the initial and injection volumes became to be the same as the each corresponding injection of IATC measurement. The titration vessel was kept at a constant temperature in a hand-made glass-bath with circulating water from a VM-150 thermostat water bath (Advantec, Tokyo, Japan). The three-point calibration with standard pH solution was used. Before and after each experiment, the pH values of standard buffer solutions of pH 2, 4, and 7 were confirmed. The observed pH values of the protein solution were corrected with the second-order polynomial function, whose coefficients were determined using the pH values of three standard solutions at the experimental temperature. The pH of the control solution without protein was measured in the manner described above.

## 2.4. Correction of the dilution heat

In the ITC experiment, the observed heat by ligand-titration to the protein solution must be corrected with the dilution heat of both the protein and the ligand. In the present study, while the dilution heat of the protein in the calorimetry cell was small enough to be ignored, that of the ligand solution in the syringe was large enough to be corrected properly in order to obtain the accurate heat effect of the protein induced by the pH change. The dilution heat of HCl-titration to the solution without protein (control experiment) was monitored in the same manner as that to the protein solution and found to depend remarkably on the pH of the solution to be titrated; that is, at lower pH, the heat of dilution became smaller. It is reasonable that the dilution heat by the concentrated ligand titration was dependent on the concentration of the ligand in the solution to be

titrated, and that the heat became smaller when the difference in concentration between these two solutions decreased. Therefore, it is important to correct the observed heat from the sample experiment by the dilution heat of the control experiment at the same pH as being compared in Fig. 3.

In order to obtain the interpolated or extrapolated value from the control experiment, a simple theoretical model was used to evaluate the pH dependence of the dilution heat in this study. Considering that the heat of dilution was the enthalpy change produced by mixing two solutions, we assumed that the enthalpy of the solution was derived mainly of the proton molar enthalpy, that the molar enthalpy could be approximated by a single power function of the proton concentration, and that the pH provides a good approximation of the logarithm of the proton concentration. Based on these assumptions, the dilution heat,  $\Delta H_{\text{dil}}$ , by mixing  $m_1$  moles of the pH<sub>1</sub> solution with  $m_2$  moles of the pH<sub>2</sub> solution was estimated by the following equation:

$$\Delta H_{\text{dil}} = H(\text{pH}_3)(m_1 + m_2) - [H(\text{pH}_1)m_1 + H(\text{pH}_2)m_2], \quad (2)$$

where pH<sub>3</sub> is the pH of the mixed solution and  $H(\text{pH})$  is the molar enthalpy of the proton in the solution. The proton molar enthalpy was simply approximated as the following function:

$$H(\text{pH}) = H_0[\text{H}^+]^c = H_0 10^{-c\text{pH}}, \quad (3)$$

where  $[\text{H}^+]$  is the proton concentration, and  $H_0$  and  $c$  are the two-adjustable parameters in this model to be determined to fit the experimental value of the dilution heat. A FORTRAN program was created in-house using a non-linear least-squares program package, SALS [30], to determine the parameters by fitting.

### 2.5. Two-state analysis of the enthalpy function

First the enthalpy as a pH function of a protein molecule,  $H(\text{pH})$ , was analyzed by a simple two-state model. Assuming the pH functions for the

native and denatured states,  $H_N(\text{pH})$  and  $H_D(\text{pH})$ , from the observed enthalpy function, the molar fraction of the denatured state,  $f_D(\text{pH})$ , was calculated as:

$$f_D(\text{pH}) = \frac{H(\text{pH}) - H_N(\text{pH})}{H_D(\text{pH}) - H_N(\text{pH})}. \quad (4)$$

The Gibbs free energy change accompanying the transition,  $\Delta G(\text{pH})$ , was calculated by Eq. (5),

$$\Delta G(\text{pH}) = -RT \ln \frac{f_D(\text{pH})}{1 - f_D(\text{pH})} \quad (5)$$

where  $R$  and  $T$  are the gas constant and the absolute temperature of the experiment, respectively.

In the non-linear least-squares fitting process, the enthalpy function of each state and the Gibbs free energy change were described by the following equations, Eqs. (6)–(9), using seven fitting parameters,  $a_N$ ,  $b_N$ ,  $c_N$ ,  $c_D$ ,  $n$ ,  $k$ , and pH<sub>d</sub>:

$$H_N(\text{pH}) = a_N \exp(-b_N \text{pH}) + c_N \quad (6)$$

$$H_D(\text{pH}) = c_D \quad (7)$$

$$\Delta \nu(\text{pH}) = n \exp(-k \text{pH}) \quad (8)$$

$$\begin{aligned} \Delta G(\text{pH}) &= (\ln 10) RT \int_{\text{pH}_d}^{\text{pH}} \Delta \nu(\text{pH}) d\text{pH} \\ &= \frac{(\ln 10) RT n}{k} \\ &\quad \times \{\exp(-k \text{pH}_d) - \exp(-k \text{pH})\}. \end{aligned} \quad (9)$$

That is, the three parameters,  $a_N$ ,  $b_N$ , and  $c_N$ , were used to express the apparent pH dependence of the native enthalpy, and the enthalpy of the denatured state was approximated by a constant,  $c_D$ . Three parameters,  $n$ ,  $k$ , and pH<sub>d</sub>, were necessary to describe the pH dependence of the Gibbs free energy change. Theoretically, the pH dependence derived from the change of proton binding-number to a protein molecule accompanying the phase transition. A theoretical function by the two-

state transition was given from the definitions of Eqs. (6) and (7) as:

$$H(\text{pH}) = H_{\text{N}}(\text{pH})[1 - f_{\text{D}}(\text{pH})] + H_{\text{D}}(\text{pH})f_{\text{D}}(\text{pH}), \quad (10)$$

where the molar fraction of the denatured state,  $f_{\text{D}}(\text{pH})$ , was calculated from the Gibbs free energy change of Eq. (9) as:

$$f_{\text{D}}(\text{pH}) = \{1 + \exp[\Delta G(\text{pH})/RT]\}^{-1}. \quad (11)$$

A fitting program was developed in-house to determine the adjustable parameters to fit the experimental data with the non-linear least-squares package, SALS [30].

#### 2.6. Joint method for the enthalpy functions obtained from two sets of titration using different HCl concentrations

In order to obtain a high data density of the enthalpy function over a wide range of pH and to check the independence of the results on the titrated HCl condition, two acid-titrations using 50 and 500 mM HCl solutions rather than 200 mM HCl solutions were also performed. For the titration with 50 mM HCl, the enthalpy was evaluated by pH steps in the range of pH 7.0–4.0, which was smaller than the range for the titration with 200 mM HCl, but did not reach below pH 2.0 after the total injection up to 150  $\mu\text{l}$ . On the contrary, in the case with 500 mM HCl, the enthalpy was observed to pH 1.5, but no details of the enthalpy change in the range of pH 7.0 to 4.0 were observed. Therefore the enthalpy function in the wide pH range was evaluated by combining the two enthalpy functions. All the corrected heats of titration of the lower concentration of HCl were adopted, and only a portion of the corrected heats of the higher concentration were adopted below the final pH of the lower concentration to calculate the enthalpy function.

#### 2.7. Circular dichroism spectroscopy

Far ultraviolet circular dichroism (CD) spectra from 205 to 255 nm were measured at pH 1.47,

2.85, and 6.57 with a J-600 spectropolarimeter (Jasco, Tokyo, Japan) using a 5 mm path-length quartz cell. The temperature of the cell was controlled by circulating the water around the cell holder from a RC6 thermostat water bath (Lauda, Germany). The molar ellipticity  $[\theta]$  was evaluated with the observed concentration by a spectrophotometer as described above. The molar ellipticity at 236 nm was monitored in the pH range from 7.0 to 1.5 at 40 °C by titrating 50 mM and 500 mM HCl to the protein solution using a 1.0 cm path-length cuvette. The reversibility of the transition was checked by measuring the far- and near-UV CD spectra after the pH of the solution was returned to 6. These spectra agreed well with those of the native state, indicating the full reversibility.

#### 2.8. Differential scanning calorimetry

Differential scanning calorimetry (DSC) experiments of ribonuclease A were performed using a highly sensitive VP-DSC (Microcal, MA, USA). The lyophilized powder of the protein was dissolved in pH 2.7, 20 mM glycine/HCl buffer, and dialyzed in the manner described above. The protein concentration was determined by a spectrophotometer using the procedure described above. The scan rate was 0.5 °C/min. The apparent heat capacity was analyzed with a two-state analysis and non-linear least-squares method as reported previously [15,16]. In the present analysis, the heat capacity functions for the native and the denatured states were approximated by linear functions of temperature.

### 3. Results

#### 3.1. Acid-titration of bovine ribonuclease A at 40 °C

As shown in Fig. 1, three protocols of injection volume were used in the acid-titration of bovine ribonuclease A at 40 °C. In the first, 200 mM HCl was titrated in 0.5  $\mu\text{l}$  increments to decrease the pH from its initial value to 2.8; in the second, 2.5  $\mu\text{l}$  aliquots were titrated to decrease the pH from 2.8 to 1.9; and in the third, 15  $\mu\text{l}$  aliquots were titrated to decrease the pH from 1.9 to the final

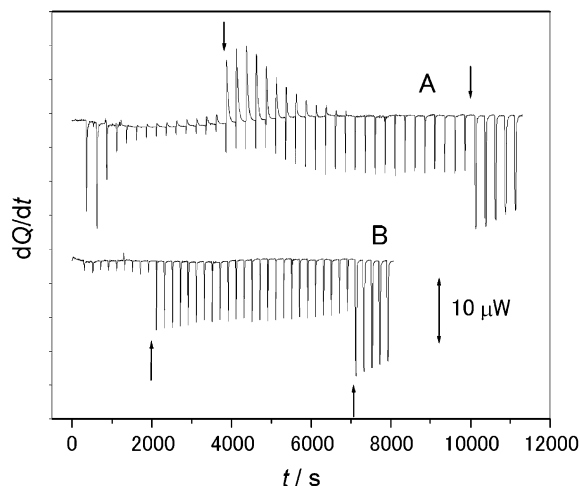


Fig. 1. (a) Typical raw calorimetry data of acid-titration to bovine ribonuclease A in 20 mM NaCl solution. In this experiment, 200 mM HCl in 20 mM NaCl was titrated to the protein solution in the calorimeter cell at 40 °C. 0.5  $\mu$ l of 200 mM HCl was added for the initial 14 injections, 2.5  $\mu$ l was added for the next 25 injections, and 15  $\mu$ l was added for the final 5 injections. The downward-pointing arrows indicate the time points at which the injection volume was changed. (b) A control titration of 200 mM HCl in 20 mM NaCl solution to 20 mM NaCl solution at 40 °C. The titration was performed with injection of 0.5, 2.5 and 15  $\mu$ l each of an HCl titrant with a syringe of 250  $\mu$ l. The upward-pointing arrows show the time points at which the injection volume was changed.

pH value. In the initial stage of the titrations, the exothermic reactions accompanying the titration were observed. After several injections of 0.5  $\mu$ l HCl solution, a small and broad endothermic peak appeared after the sharp exothermic peak in each injection. The endothermic peak became increasingly larger in the later injections and reached a maximum at the third injection after the injection volume was changed from 0.5 to 2.5  $\mu$ l. After this injection, the exothermic peaks decreased gradually, and only the exothermic peaks were observed in the final stage of the titration. The shape of the rapid exothermic peaks was similar to that of the blank titration in Fig. 1b, suggesting that the exothermic heat was produced mainly by the heat of the acid dilution. As the broader endothermic peaks were only observed in the sample titration, they were considered to be produced by the protein molecules. The reaction heat values of each acid-

titration were obtained by integrating the peak areas of each injection. The amounts of heat were plotted against the logarithm of the total calculated concentration of injected HCl in the calorimeter cell, as shown in Fig. 2a. In the protein solution, the heat effects were negative in the range of more than 3.25 of  $-\log\{[\text{HCl}]/M\}$ , and became in the range of  $-\log\{[\text{HCl}]/M\}$  from 3.0 to 2.25. In the range below 2.25, negative heat effects identical to those in the control experiment were observed, indicating that the heat of the protein solution was equivalent to the heat of dilution in the denatured state. In the control experiment without protein, the heat effects were negative throughout the range of  $-\log\{[\text{HCl}]/M\}$ . The heat values from the protein solution agreed with the amounts of heat from the control experiment under the condition under 2.25 of  $-\log\{[\text{HCl}]/M\}$ .

Because the protein stability and dilution heat are considered to depend on pH, it is important to measure the pH of the solutions experimentally. Fig. 2b shows the results of the pH measurements of both the protein and control solutions titrated with several volumes of 200 mM HCl. The pH was plotted against  $-\log\{[\text{HCl}]/M\}$ . From this figure, it is clear that some parts of the injected protons were bound to the protein, resulting in the deviation of the pH of protein solution in the pH range above pH 2.0.

In Fig. 3, in order to evaluate the pH dependence of the heat effect for both the protein solution and control experiment, we plot the heat by each injection from Fig. 2a and b against the pH. In the protein solution, positive heat effects were observed in the pH range from 4.5 to 2.5, and they reached a maximum at about pH 3.0. In the case of the control experiment, all the heats were negative due to the dilution heat with HCl solution. Not surprisingly, the dilution was dependent on the pH of the solution.

We found that the pH dependence was well explained by the simple theoretical model described in the Section 2. In fact, the solid lines, based on this model, explained the control experiment very well, as shown in Fig. 3, while only two fitting parameters of this model,  $H_0$  and  $c$  in Eq. (3), were required adjustment to fit the experimental data. From both the good agreement to the

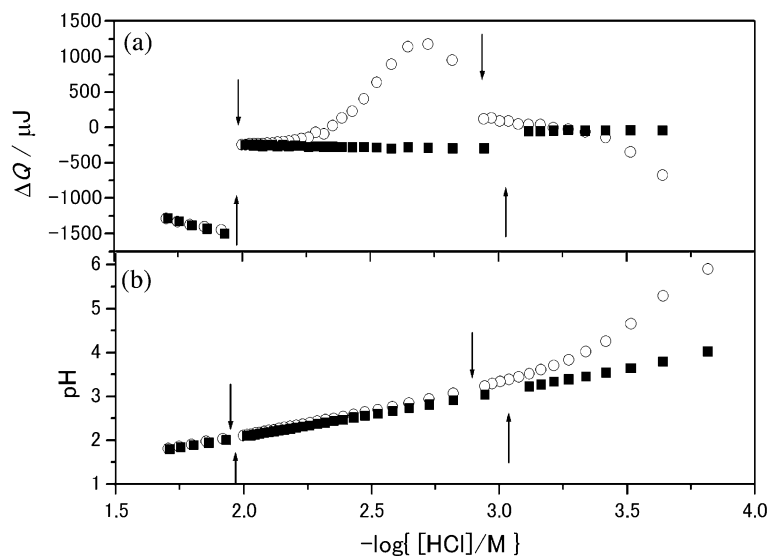


Fig. 2. (a) Acid-titration heat effects of the protein solution ( $\circ$ ) and those of the control ( $\blacksquare$ ), evaluated as the total area of each injection in Fig. 1. The arrows show the time points at which the injection volume was changed. The total concentration of added HCl was calculated and plotted as the horizontal axis in the normal logarithmic scale. (b) The pH measurement of acid-titration to bovine ribonuclease A ( $\circ$ ) with 200 mM HCl in 20 mM NaCl at 40 °C and that to 20 mM NaCl solution as a control experiment ( $\blacksquare$ ). The titration was performed to the 10 ml of solution in the thermostat cell with 3.7, 18, and 110  $\mu\text{l}$  of the HCl solution.

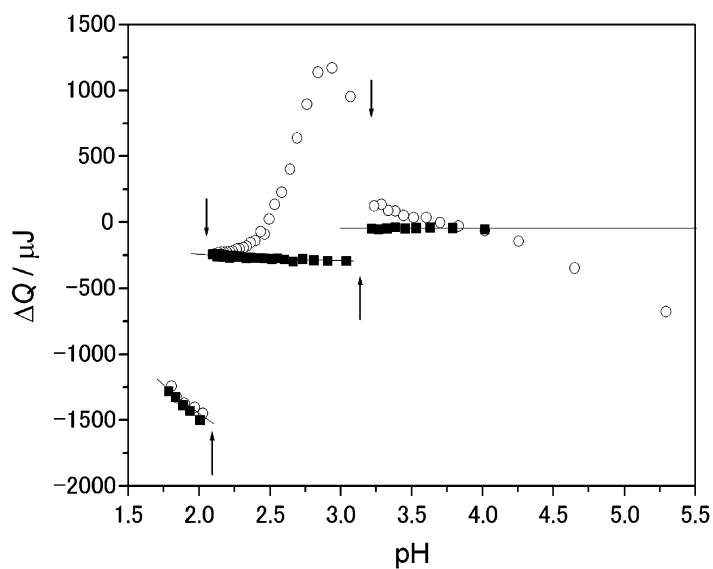


Fig. 3. The pH dependence of the heat effects of HCl-titration to ribonuclease A solution ( $\circ$ ) and those to the solution without protein (the control experiment,  $\blacksquare$ ), evaluated with the data in Fig. 2a and b. The arrows indicate the time points at which the injection volume was changed. The solid lines are the best-fitted theoretical functions for the control data, calculated with Eqs. (2) and (3).



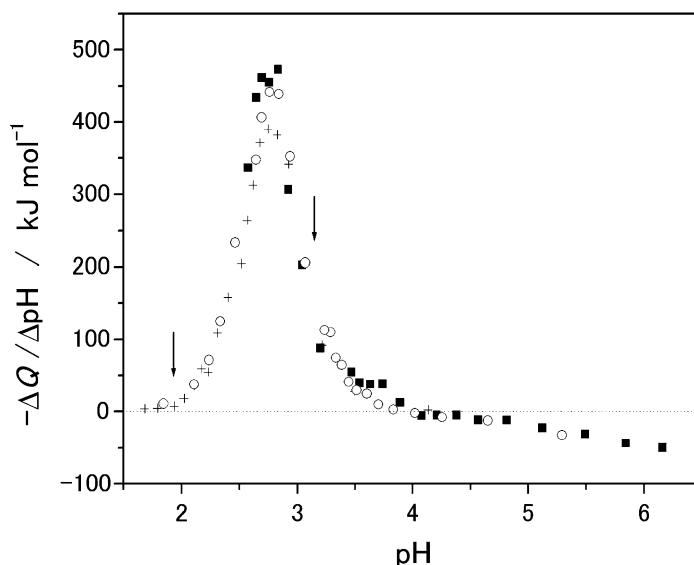


Fig. 4. The pH dependence of the heat effects induced by the pH change,  $-\Delta Q/\Delta pH$ , of ribonuclease A with 200 mM HCl ( $\circ$ ), evaluated with the data in Fig. 4. The arrows indicate the time points at which the injection volume was changed. The heat values obtained in the same manner by the titration with 50 mM HCl ( $\blacksquare$ ) or 500 mM HCl (crosses) are also plotted. The dotted line indicates zero level.

experimental data and the low freedom of the fitting function, not only the interpolation but also the extrapolation of the theoretical curve was expected to be reliable for use in determining correction of the dilution heat.

By subtracting the dilution heat evaluated at the same pH, the heat effects of the protein molecule induced by the acid-titration could be evaluated. Because these effects were induced by the pH change produced by the acid titration, we drew a new plot (Fig. 4) to compare the heat effects among several experiments with different experimental conditions, such as using different injection volumes or using different acid concentrations. Because the enthalpy of the protein molecule is a state function, in theory it should be independent of the volumes and acid concentration. Because the pH change,  $\Delta pH$ , and the heat effects,  $\Delta Q$ , induced by the pH change were observed directly by isothermal titration calorimetry and pH measurement, the ratio of these observable values,  $-\Delta Q/\Delta pH$ , can also be obtained directly as an approximation of  $-(\partial H/\partial pH)_T$ .

The open circles in Fig. 4 show the experimental

values obtained by several injection volumes of 200 mM HCl. A clear and almost symmetrical pH function with a maximum,  $460 \text{ kJ mol}^{-1}$ , at pH 2.6 was evaluated by this plot. By the same procedure,  $-\Delta Q/\Delta pH$  with different acid concentrations, such as 50 mM and 500 mM HCl, were plotted together in this figure. This figure indicates that the results by various acid concentrations almost agreed with each other, although a slight deviation in the case of the data with 500 mM HCl-titration was observed around pH 2.6, where the values reached the maximum. This slight deviation was caused by the slight diffusive leakage of the concentrated acid from the injection syringe. By using an acid of lower concentration, the contribution of the leakage can be suppressed, and the pH change in the neutral pH range can be reduced. However, the final pH was increased by using an acid of lower acid concentration, and the acid unfolding of ribonuclease A was not completed by the 50 mM HCl titration, as shown in Fig. 4.

In order to overcome this problem and to render this method more flexible, we combined the two

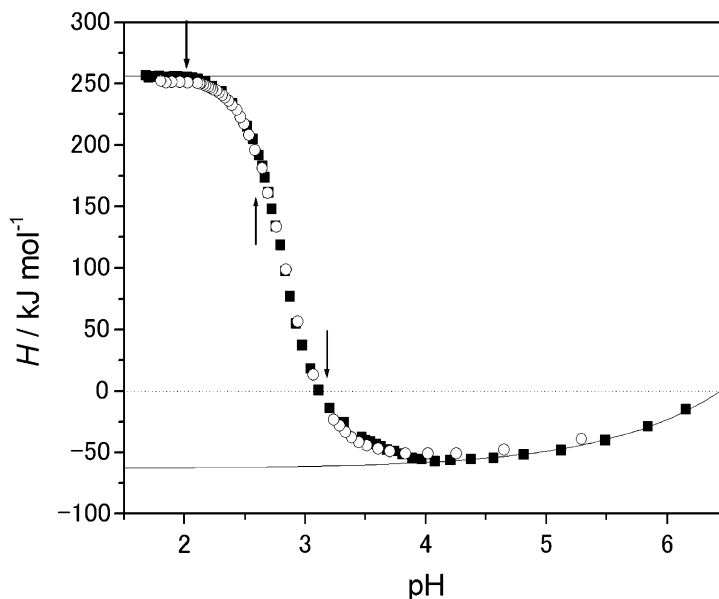


Fig. 5. The enthalpy function of bovine ribonuclease A between pH 6.5 and 1.5 at 40 °C by isothermal acid-titration calorimetry. Data from the titration with 200 mM HCl are plotted as open circles. The downward-pointing arrows indicate the time points at which the injection volume was changed. The enthalpies by the joint method using both 50 and 500 mM HCl are plotted as filled squares. The upward-pointing arrows show the time points at which the two-enthalpy functions were joined by the titration with 50 or 500 mM HCl. The solid lines show the fitted function for the native state, approximated as an exponential function, and that for the denatured state, approximated as a constant value obtained as an average enthalpy in the range of pH 2.0~1.7.

sets of titrations with different acid concentrations as described in the Materials and Methods. As seen in Fig. 4, the data in the low pH region did not depend on the acid concentration, and the data of low concentration can be connected safely to the high concentration in this pH region.

In Fig. 5, the enthalpy by only 200 mM HCl titration was compared to the enthalpy by combining the two sets of titrations using 50 and 500 mM HCl. The good agreement of these two functions indicates that the enthalpy obtained by this method was independent of the HCl concentration used, and that the joint method works well. In the enthalpy by the joint method, there were more data points with smaller pH steps in the higher pH region, and the data can also be evaluated to the lower pH region.

The enthalpy decreased by decreasing the pH from 6.5 to 4.0, in which range the protein was in the native state, as shown by CD measurement in the following. This pH dependence was found to

be well explained by an exponential function as in Fig. 5. In the pH region lower than 4.0, the enthalpy increased rapidly by decreasing pH, and it became constant below pH 2.0, in which range the protein was in the acid-denatured state, as confirmed by CD measurement.

By assuming a constant value for the enthalpy function of the denatured state and an exponential function for that of the native state, and by extrapolating these functions to the transition pH around pH 2.6, the enthalpy change by the unfolding was estimated as approximately 310 kJ/mol at pH 2.8 and 40 °C. This enthalpy change can be obtained correctly without any assumption on the cooperativity of the transition, and it can be considered a calorimetric enthalpy as in the case of differential scanning calorimetry [15].

Based on the extrapolation of enthalpy functions for the native and the denatured states, a two-state analysis was performed as described in the Section 2, and the results are plotted in Fig. 6. The

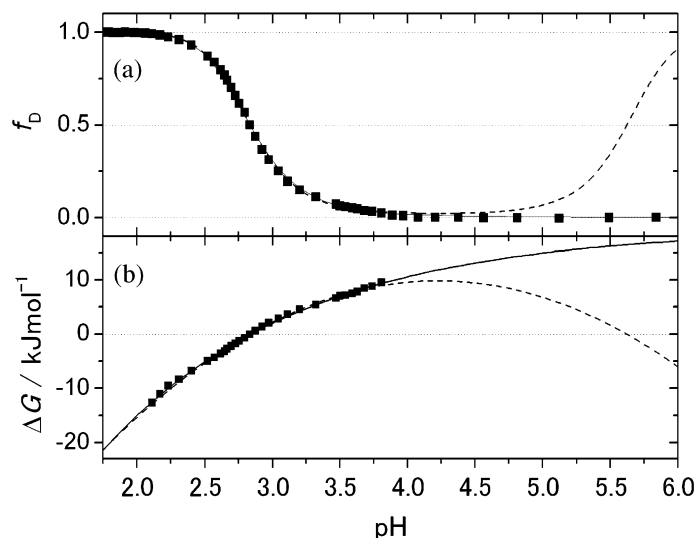


Fig. 6. The pH dependence of the molar fraction of the denatured state (a) and Gibbs free energy change (b) calculated from the enthalpy functions in Fig. 5 by two-state analysis. The Gibbs free energy change was fitted with an exponential function (solid line) and a second-order polynomial function (broken line) in panel b. The molar fraction of the denatured state was calculated based on the fitted exponential (solid line) and the second-order polynomial (broken line) in panel a.

evaluated Gibbs free energy change was clearly a curved function, and could not be fitted by a linear function, indicating that more than two parameters were necessary to explain the experimental data. If simply the second-order polynomial function with three adjustable parameters were fitted to the data, the extrapolated Gibbs free energy would indicate the alkaline unfolding above pH 6, where the native state is actually more stable for this protein. However, an exponential function that also included the three fitting parameters can explain the data very well, and can be extrapolated to the neutral pH without making an artificial transition. In all the experimental data in this study, the Gibbs free energy change can be well fitted by exponential functions.

As described in the Section 2, the pH dependence of the Gibbs free energy change was caused by the change of the proton binding-number accompanying the unfolding. Therefore, the exponential dependence of the Gibbs free energy change indicates the exponential dependence of the change of proton binding-number, whose pH dependence was explained by using only two adjustable parameters: the change of proton bind-

ing-number at the midpoint pH and its pH derivative at the pH. In summary, four parameters were necessary to describe the enthalpy functions of the native and denatured states, two parameters to describe the proton binding-number change, and one parameter to describe the midpoint pH,  $\text{pH}_d$ .

The rough estimates for these seven parameters were determined as shown in Figs. 5 and 6, and refined by using non-linear least-squares fitting to the enthalpy function including acid transition. In Fig. 7, the best-fitted function was plotted to show the good agreement of the theoretical function with the experimental values at 40 °C. At 15 °C, the protein was in the native state even at pH 2.0, based on the CD and DSC data, so that the enthalpy at this temperature gave the pH dependence of the native state. In the first approximation, the native enthalpy of ribonuclease A can be explained by an exponential function, as seen in Fig. 7. At 65 °C, the protein unfolded even at pH 5, and the enthalpy of this temperature was considered to be the enthalpy of the denatured state, and well approximated by a linear function. In the present study, the native enthalpy of ribonuclease A was approximated by an exponential function.

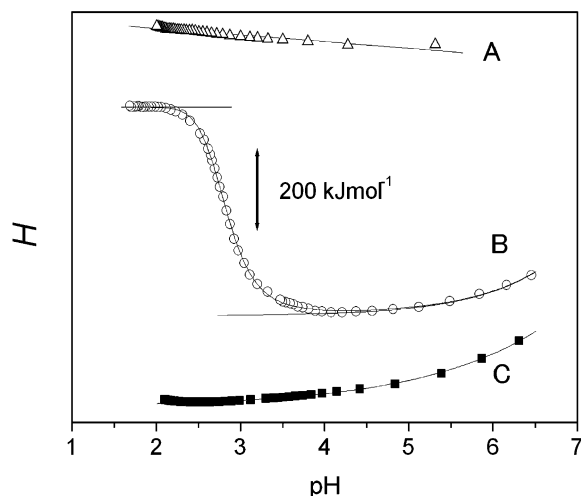


Fig. 7. The enthalpy of bovine ribonuclease A was determined as a function of pH at 15 °C (■), 40 °C (○) and 65 °C (△). The solid lines were determined by least-squares fitting with an exponential function (15 °C), a linear function (65 °C), and a theoretical curve calculated by a two-state transition model with Eq. (10) (40 °C), respectively.

For the denatured enthalpy, only a constant was used for the two-state analysis in order to avoid the over-fitting caused by introducing the unnecessary freedom to the fitting model. Only a constant value for the denatured state was needed to explain the experimental data in this study.

The thermodynamic parameters determined by the two-state analysis are summarized in Table 1. At 40 °C, the results from the single titration with

200 mM HCl were compared with those by the joint method. The good agreement of the analysis of independent experiments using different experimental conditions suggested the good precision and reproducibility of the present method.

### 3.2. Structure transition of bovine ribonuclease A monitored by far-UV CD and differential scanning calorimetry

In order to check the validity of these thermodynamic parameters, the structural change induced by acid-titration was observed by circular dichroism (CD) spectroscopy. In Fig. 8b, far ultraviolet (far-UV) CD spectra at several pHs were compared. The CD spectra of this region changed significantly by the acid-denaturation of ribonuclease A. The intensity of CD in the range from 205 to 230 nm decreased by the acid denaturation, while that in the range from 230 to 245 nm increased. In order to use the same solution as used for the calorimetry and pH measurement, the CD at 236 nm were monitored while adding HCl to change the pH of the solution. A very clear transition was observed in the same pH range, i.e. from pH 4 to 2. The solid line in this figure was fitted to the CD data using the same thermodynamic parameters as used for the transition—that is, using the  $pH_d$  and  $\Delta\nu$  obtained by IATC (Table 1). The agreement of the fitting function to the CD data confirmed that the acid-transition observed by the calorimetry was accompanied with

Table 1

The thermodynamic parameter, such as mid-point pH,  $pH_d$ , proton binding-number difference,  $\Delta\nu$ , the pH differential of proton-binding number difference,  $\left[\frac{\partial\Delta\nu}{\partial pH}\right]_T$ , enthalpy change,  $\Delta H_{ND}^{cal}$  and the pH differential of enthalpy change,  $\left[\frac{\partial\Delta H}{\partial pH}\right]_T$ , with pH transition determined by acid-titration calorimetry at 35, 40 and 45 °C

$T/(^{\circ}\text{C})$	$pH_d$	$\Delta\nu^a$	$\left[\frac{\partial\Delta\nu}{\partial pH}\right]_T^a$	$\Delta H^a$ /kJ mol <sup>-1</sup>	$\left[\frac{\partial\Delta H}{\partial pH}\right]_T^a$ /kJ mol <sup>-1</sup>	$\left[\frac{\partial H_N}{\partial pH}\right]_T^b$ /kJ mol <sup>-1</sup>
35	2.50	2.6	-1	252	-1	15
40	2.84 <sup>c</sup>	2.5 <sup>c</sup>	-2	314 <sup>c</sup>	-3 <sup>c</sup>	18 <sup>c</sup>
40	2.84 <sup>d</sup>	2.4 <sup>d</sup>	-1	309 <sup>d</sup>	-2 <sup>d</sup>	14 <sup>d</sup>
45	3.21	2.1	-1	330	0	6

(a) Evaluated at the mid point pH,  $pH_d$ , of the given temperature; (b) evaluated at pH 5.0; (c) using the data with joint method; (d) using the data without joint method.

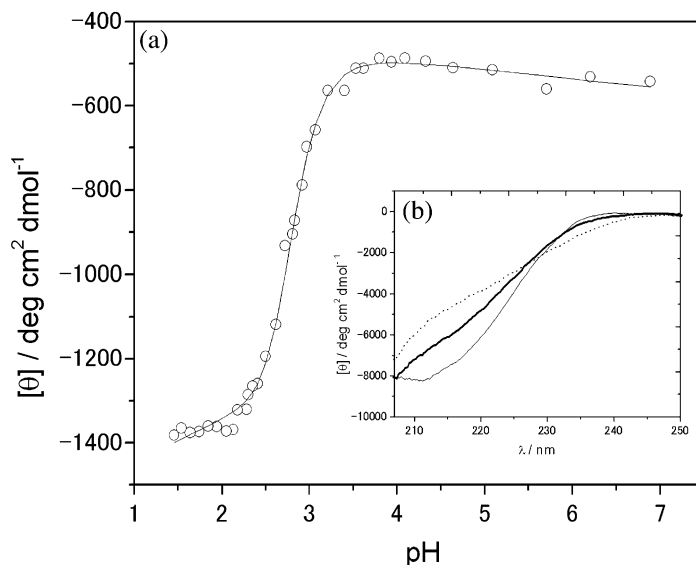


Fig. 8. (a) The pH dependence of molar ellipticity  $[\theta]$  at 236 nm of bovine ribonuclease A at 40 °C. The same protein solution was used as for isothermal acid-titration calorimetry. The solid line is the theoretical curve obtained with the best-fitted thermodynamic parameters,  $\text{pH}_d$ ,  $\Delta\nu$ , and  $\partial\Delta\nu/\partial\text{pH}$ , from Table 1. (b) Far-UV CD spectra of bovine ribonuclease A at pH 1.47 (dotted line), 2.85 (thick solid line), and 6.57 (solid line). The same protein solution was used as for isothermal acid-titration calorimetry.

the remarkable structural change, and that the thermodynamic parameters determined by IATC were appropriate to describe the transition.

The enthalpy change accompanying the pH transition observed by IATC was compared to that of the thermal denaturation determined by differential scanning calorimetry (DSC). Fig. 9 shows the temperature dependence of the partial molar heat capacity of ribonuclease A in 20 mM glycine buffer at pH 2.7. The solid line is a theoretical curve fitted to the experimental data by the non-linear least-squares method with a two-state transition model. The theoretical curve agreed very well with the experiment data, suggesting that no stable intermediate state existed during the thermal transition. The enthalpy change ( $\Delta H^{\text{cal}}$ ) determined by this analysis was  $310 \pm 3 \text{ kJ mol}^{-1}$  at the midpoint temperature (39.45 °C). It showed good agreement with the enthalpy change ( $\Delta H^{\text{cal}}$ ),  $312 \pm 3 \text{ kJ mol}^{-1}$  at 40 °C (Table 1), determined by IATC. In order to check the reversibility of the transition, the enthalpy change of the observed transition in the re-heating was compared with

$\Delta H^{\text{cal}}$ , and these ratios were found to be 0.97, indicating the good reversibility.

### 3.3. Thermodynamic parameters from IATC at various temperatures

Isothermal titration calorimetry was performed at several different temperatures in this study. In this section, we analyze the temperature dependence of the thermodynamic functions observed by IATC.

The thermodynamic parameters are presented in Table 1. It is worth noting that the changes of the thermodynamic parameters were evaluated at the midpoint pH of each temperature in order to minimize the estimation error for each parameter. Thus all of these values, with the exception of the last parameter in the table, were evaluated not only at different temperatures but also at different pH values.

Fig. 10a shows the clear temperature dependence of the enthalpy change, which has a positive slope of  $8 \pm 2 \text{ kJ K}^{-1} \text{ mol}^{-1}$ . The slope can be

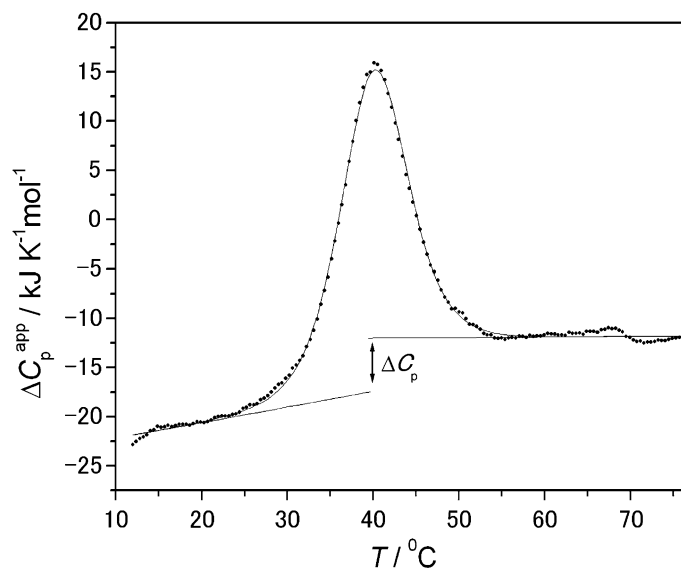


Fig. 9. The temperature dependence of the partial molar heat capacity of bovine ribonuclease A in 20 mM glycine buffer at pH 2.7 (circles). The solid line is the theoretical curve determined by non-linear least-squares fitting assuming a two-state model. The heat capacity change,  $\Delta C_p$ , at the transition temperature is also shown.

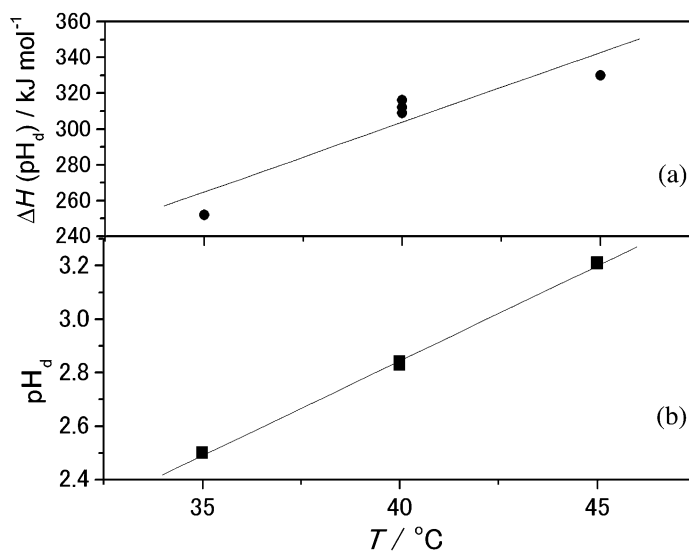


Fig. 10. (a) The temperature dependence of the enthalpy change for transition ( $\Delta H$ ) at the midpoint pH,  $pH_d$  in Table 1. The solid line is the best-fitted linear function to evaluate  $d\Delta H(T, pH_d)/dT$  as  $8 \pm 2 \text{ kJ K}^{-1} \text{ mol}^{-1}$ . (b) The temperature dependence of the midpoint pH,  $pH_d$ , in Table 1. The solid line was the best-fitted linear function to evaluate  $dpH_d/dT$  as  $0.071 \pm 0.002 \text{ K}^{-1}$ .

interpreted in the same way as the slope of the traditional plot of  $\Delta H$  vs. the midpoint temperature under various pH values in DSC analysis. Compared to the plot previously reported for this protein by DSC [20], the deviation from the linear line in Fig. 10a does not seem particularly large. As discussed in that report [20], many different slopes of the same kind of linear line have been reported for this well-studied protein, indicating that certain unknown factors may contribute to the observed deviation. Further studies will be needed to clarify this matter.

The temperature dependence of  $pH_d$  in Fig. 10b in the range from 35 to 45 °C can be well approximated by a simple linear function. The most probable value and the estimation error for the value for  $dpH_d/dT$  at 40 °C was determined as  $0.071 \pm 0.002 \text{ K}^{-1}$  by the linear fitting.

From the equation on the definition of the midpoint pH,  $pH_d$ , at a given temperature,  $T$ , the next equation holds:

$$\Delta G[T, pH_d(T)] = 0. \quad (12)$$

We get the following equation by differentiating the above equation by temperature:

$$-\Delta S[T, pH_d(T)] + \frac{\partial \Delta G}{\partial pH} \frac{dpH_d}{dT} = 0. \quad (13)$$

We can then derive the equation:

$$\Delta H[T, pH_d(T)] = (\ln 10) RT^2 \Delta v [T, pH_d(T)] \frac{dpH_d}{dT} \quad (14)$$

by using the following two relations,

$$\Delta H[T, pH_d(T)] - T \Delta S[T, pH_d(T)] = 0,$$

$$\frac{\partial \Delta G}{\partial pH} = (\ln 10) RT \Delta v.$$

The enthalpy change in the left-hand side of Eq. (14) can be designated the ‘van’t Hoff enthalpy,’ because it was derived from the temperature

dependence of the Gibbs free energy change. This equation indicates that the van’t Hoff enthalpy can be easily evaluated from the results of IATC at several temperatures.

In the case of ribonuclease A at 40 °C, the van’t Hoff enthalpy was calculated as  $330 \pm 20 \text{ kJ mol}^{-1}$ , which agreed with the calorimetric enthalpy,  $\Delta H_{ND}^{cal}$ ,  $312 \pm 3 \text{ kJ mol}^{-1}$ , obtained directly by IATC at 40 °C. The agreement of the calorimetric and the van’t Hoff enthalpies strongly indicates that the assumed two-state model to analyze the enthalpy function was valid and no stable intermediate state appeared during the pH transition of this protein.

As previously discussed [21], the heat capacity change of the thermal transition under constant pH and pressure can be evaluated from the  $T_m$  dependence of the observed enthalpy change at several  $pH_d$ ,  $d\Delta H/dT_m$ , the pH dependence of the enthalpy under constant temperature,  $(\partial \Delta H / \partial pH)_T$ , and the pH dependence of  $T_m$ ,  $dT_m/dpH$  as:

$$\Delta C_p = \frac{d\Delta H(T_m, pH)}{dT_m} - \left( \frac{\partial \Delta H}{\partial pH} \right)_T \frac{dT_m}{dpH}. \quad (15)$$

This equation was derived for DSC analysis, and in many cases the heat capacity change was evaluated under the assumption that the second-term of the right-hand side of this equation was negligible, since DSC cannot be used to evaluate the pH dependence of the enthalpy change at constant temperature. However, a similar equation that is applicable to the results of IATC could be derived as:

$$\Delta C_p = \frac{d\Delta H(T, pH_d)}{dT} - \left( \frac{\partial \Delta H}{\partial pH} \right)_T \frac{dpH_d}{dT}. \quad (16)$$

Since IATC can be used to evaluate all three dependences in the right-hand side of this equation, the heat capacity change can be calculated without neglecting the second term. In the case of ribonuclease A in this study, however, the magnitude of the second-term was found to be less than the experimental error of the first term, and thus the heat capacity change had to be calculated using only the first term. The resulting value,  $8 \pm 2 \text{ kJ}$

$\text{K}^{-1} \text{mol}^{-1}$ , agreed with the heat capacity change obtained from a single DSC run in Fig. 9,  $5.5 \pm 0.9 \text{ kJ K}^{-1} \text{mol}^{-1}$ , within the experimental error.

## 4. Discussion

### 4.1. Evaluation and correction of pH-dependent dilution heat by acid-titration

Since the dilution heat of acid was not negligible, it was necessary to observe the pH of the protein solution in the cell, and to evaluate the dilution heat at the same pH. To interpolate or extrapolate the data from the control titration, a simple model with only two adjustable parameters was used, as shown in Eq. (3). This simple model explained the pH dependence of the observed dilution heat in Fig. 3 very well, even when the injection volume was changed. Although, in place of this model, the polynomial functions of pH can be used to fit the control titration [23], the extrapolation tends to become unstable if the fitting model has a large number of adjustable parameters to be determined. Because the extrapolation of dilution heat in the neutral pH is important for the correction, the simple model with only two adjustable parameters proposed in this article is expected to be effective in the analysis.

### 4.2. Avoiding the neutralization heat in acid-titration calorimetry

While the dilution heat of acid and also that of alkaline (data not shown) can be corrected precisely by using the currently available isothermal titration calorimetry, the neutralization heat was large enough to make it difficult to observe the enthalpy change of protein molecule separately from the heat. Therefore, it is necessary to do the acid-titration calorimetry under the low concentration of  $\text{OH}^-$ . Thus, it may become difficult to do the acid-titration calorimetry under high pH such as above pH 10.

In the case of alkaline-titration calorimetry, the neutralization heat becomes severe problem in the acid pH region because of the high concentration of proton, and even in the alkaline pH because the proteins release the protons by alkaline-titration,

producing the large neutralization heat. Because the general ligand to protein molecules is not  $\text{OH}^-$  but  $\text{H}^+$ , the acid-titration does not induce the release of  $\text{OH}^-$  generally and only the proton binding can be observed.

### 4.3. Analysis of the enthalpy function of protein at a fixed temperature

As in the previous studies of lysozyme [22] and apomyoglobin [23], the enthalpy of the native state of ribonuclease A decreased with decreasing pH, as shown in Figs. 5, 7 and 11. In this study, a simple exponential function of pH could explain the pH dependence very well at each temperature, and the extrapolation toward more acidic pH region was judged to be valid based on the agreement between the values from the DSC and the van't Hoff analysis.

For the enthalpy function of the acid-denatured state below pH 2, we found no clear pH dependence. Based on the facts that almost all the amino acids in the denatured state were already protonated in this acidic region, and that the protonation enthalpy of the carboxyl group was very small, our finding of a lack of pH dependence seems reasonable. A constant enthalpy was assumed for all the acid-denatured to analyze the pH transition, and was found to explain the experimental data very well. The extrapolation to the midpoint pH in the transition region was also considered to be accurate judging from the agreement with other measurements.

When the enthalpy functions for the native and denatured states are estimated, the enthalpy change between these states can be evaluated directly without assuming the mechanism of the transition. Calorimetry was used as a unique method to observe the enthalpy directly, and acid-titration calorimetry allowed us to determine the enthalpy change of pH transition as well as the pH dependence of the enthalpy change.

### 4.4. pH dependence of Gibbs free energy change

In order to analyze the data in the pH transition region, an important pH dependence to be considered that of the Gibbs free energy change. Because



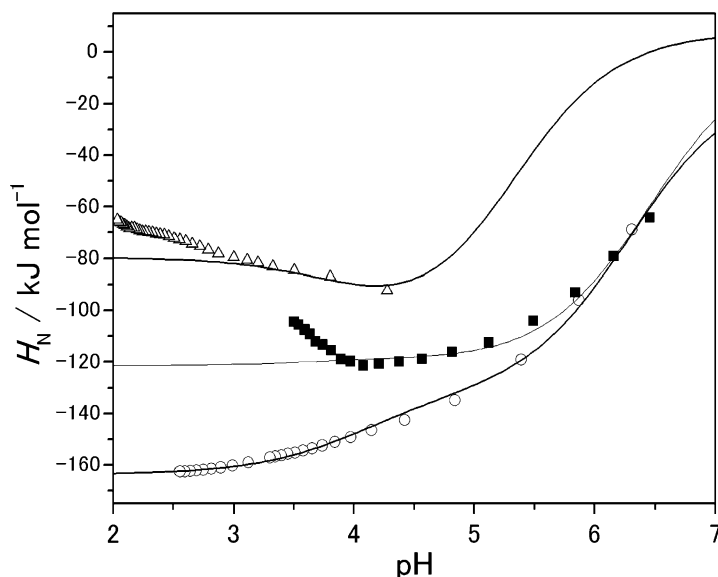


Fig. 11. The enthalpy function of ribonuclease A at 15 °C (circles), 40 °C (squares), and 65 °C (triangles). The solid lines are the theoretical curves of protonation enthalpy. In this calculation, the deprotonation enthalpy, the deprotonation heat capacity and  $pK_a$  for glutamic acid, aspartic acid and histidine were from Table 2 except for the  $pK_a$  for histidine at 15 and 40 °C because the histidines in the native state were reported to have abnormal  $pK_a$  [31–33]. The  $pK_a$ s for histidine at these temperatures were determined to fit the experimental data. In this calculation, while all of the five aspartic acids, the five glutamic acids, one C-terminal carboxyl group and four histidines were considered in the denatured state, the protonation of three aspartic acids was neglected in the native state, under the assumption that these have abnormally low  $pK_a$  values. The thermodynamic parameters for the C-terminal carboxyl group were estimated to be the same as those for aspartic acid in this calculation.

the dependence could be theoretically derived from the binding-number difference between the two states,  $\Delta\nu_{ND}$ , and because this difference was considered to be largely dependent on pH, it was necessary to consider the second-order pH dependence of the Gibbs free energy change, as shown in Fig. 6b. The figure indicates that the curvature of the Gibbs free energy change was negative and that the function was well approximated by an exponential function of pH using three adjustable parameters. Although a second-order polynomial function that also has the three adjustable parameters can fit the data, the extrapolation of the function predicted an abnormal destabilization of the native state at the neutral pH, where the native state was actually more stable. While additional higher order polynomial functions can explain the data near the pH transition, the extrapolation of these functions becomes unstable because of their large numbers of adjustable parameters, which

would decrease the reliability of the model. Therefore, the simple exponential function of pH was used to analyze the experimental data in this study. In addition, the Gibbs free energy change determined from the IATC data can also explain the pH transition observed by CD measurement, as seen in Fig. 8, indicating the validity of the model.

#### 4.5. The pH-dependence of the enthalpy function of each thermodynamic state was almost explained by the protonation enthalpy of carboxyl groups and histidines

At 15 °C, the enthalpy changed by approximately 100 kJ/mol in the pH range from 6.5 to 2, as seen in Fig. 7. The main factor affecting enthalpy change in the native state was considered to be the protonation enthalpy with carboxyl groups and histidines, as reported previously [23]. The bovine pancreas ribonuclease A has five glutamic acids,

Table 2

Thermodynamic parameters for the deprotonation of the side chains of aspartate, glutamate, and histidine

	Glutamic acid	Aspartic acid	Histidine
$\Delta H_{\text{deprot}}$ (25 °C)/kJ mol <sup>-1</sup>	1.6	4.0	30.0
$\Delta C_p$ /kJ K <sup>-1</sup> mol <sup>-1</sup>	-0.155	-0.150	0.016
pK <sub>a</sub> (25 °C)	4.27	3.87	6.00
$\frac{\partial \text{p}K_a}{\partial T}$	-0.00094	-0.00235	-0.01763

Data for the deprotonation enthalpy,  $\Delta H_{\text{deprot}}$ , and pK<sub>a</sub> were taken from the study by Izatt and Christensen [34]. Data for the deprotonation heat capacity of glutamic acid and aspartic acid were calculated using this data. Data for the heat capacity change of histidine were taken from the previously published data for imidazole [35]. The values for  $\frac{\partial \text{p}K_a}{\partial T}$  were calculated with the deprotonation enthalpy derived from Eq. (17).

five aspartic acids, one carboxyl-terminal group, and four histidines in a molecule. The solid lines in Fig. 11 are the approximation curves of the protonation enthalpies of these groups in the native state at 15 °C and 40 °C, and that in the denatured state at 65 °C. Table 2 shows the protonation enthalpies of glutamic acid, aspartic acid, and histidine used in these calculations. The temperature dependence of pK<sub>a</sub>,  $\frac{\partial \text{p}K_a}{\partial T}$ , was calculated with the deprotonation enthalpy using Eq. (17):

$$\frac{\partial \text{p}K_a}{\partial T} = \frac{\Delta H_{\text{deprot}}}{(\ln 10)RT^2} \quad (17)$$

The pK<sub>a</sub> values of these groups at the given temperature were calculated considering  $\frac{\partial \text{p}K_a}{\partial T}$ .

The deprotonation enthalpy and pK<sub>a</sub> of the carboxyl group of the C-terminal were assumed to be the same as those of aspartic acid.

Considering the previous report that at least one residue—i.e. an Asp—of ribonuclease A has an abnormally low pK<sub>a</sub> [31–33], we assumed that three or more aspartic or glutamic residues, including this Asp, should have abnormal pK<sub>a</sub> values in the native state, because the proton binding-number change in this pH region was found to be more than 2, as shown in Table 1. We therefore assumed that three carboxyl groups had abnormally low pK<sub>a</sub> values of less than 2, and that the other three carboxyl groups of aspartic acid and the C-terminal had normal pK<sub>a</sub> values. Because some of

the histidines have also been reported to have abnormally high pK<sub>a</sub> values in the native state [31–33], the pK<sub>a</sub> values of histidines were adjusted to fit the experimental data in Fig. 11. The best-fitted pK<sub>a</sub> values, 6.3 at 15 °C and 6.5 at 40 °C, were considered to be reasonable values for the pK<sub>a</sub> for histidine in the native state. In Fig. 11, the calculated lines were almost consistent with the experiment data, indicating that the enthalpy functions of both the native and denatured state were explained by the protonation enthalpy of the residues.

#### 4.6. The van't Hoff enthalpy from IATC

The van't Hoff enthalpy was calculated using the temperature dependence of the midpoint pH, pH<sub>d</sub>, and the proton binding-number change,  $\Delta \nu$ , as shown in Eq. (14). In the case of ribonuclease A at 40 °C, both the parameters can be determined with rather small experimental error. Therefore, the van't Hoff enthalpy at 40 °C was determined (with a small estimation error) to be  $330 \pm 20$  kJ mol<sup>-1</sup>, which agreed with the directly observed enthalpy change of  $312 \pm 3$  kJ mol<sup>-1</sup> at this temperature. To the best of our knowledge, this is the first report to prove the validity of the two-state transition induced by pH by comparing the calorimetric and van't Hoff enthalpy, which was established as a standard procedure in the DSC analysis. As indicated in this case, the temperature dependence in the range of 10 K is sufficient to determine the van't Hoff enthalpy by using Eq. (14), and it is also necessary to determine  $\Delta \nu$

accurately in this temperature range by using an appropriate thermodynamic model, as discussed above.

4.7. *The contribution of the pH differential of enthalpy change,  $\left(\frac{\partial \Delta H}{\partial \text{pH}}\right)_T$ , to the heat capacity change,  $\Delta C_p$*

As discussed in the Section 1, the heat capacity change of thermal transition has traditionally been determined as the slope of the plotting of  $\Delta H(T_m)$  vs.  $T_m$  without consideration of the pH dependence of the enthalpy change. Because the pH dependence of the enthalpy change can be determined by the IATC method, it is expected that this method can also accurately determine  $\Delta C_p$  by means of Eq. (16). If the pH dependence of the enthalpy change is not negligible, it is necessary to reexamine the heat capacity changes reported in many previous works. To our knowledge, this is the first report to determine the pH dependence of the enthalpy change, and our results indicate that the pH dependence might be negligible in the transition of ribonuclease A in the acidic region, because the magnitude of the correction term for the heat capacity change derived from the pH dependence was  $0.2 \text{ kJ K}^{-1} \text{ mol}^{-1}$ , which can be neglected in this case.

We note that this result does not mean that the pH dependence of the enthalpy change will always be negligible. From the pH dependence of the enthalpy function of a protein, it was suggested that the pH dependence of the native enthalpy becomes larger under neutral pH than under an acidic condition. If the pH dependence of the denatured enthalpy does not become larger under neutral pH, the pH dependence of the enthalpy change between the native and the denatured state will become larger enough to contribute to the heat capacity evaluation.

4.8. *The pH dependence of the heat capacity of the native state*

The pH dependencies of the native state enthalpy,  $(\partial H / \partial \text{pH})_T$ , at pH 5.0 are listed in Table 1. These values at several temperatures clearly indi-

cate the existence of temperature dependence. These results suggest that the pH dependence of the heat capacity change of the native state protein, according to Eq. (18), is  $-0.9 \pm 0.6 \text{ kJ K}^{-1} \text{ mol}^{-1} \text{ pH}^{-1}$ .

$$\frac{\partial}{\partial T} \left( \frac{\partial H}{\partial \text{pH}} \right) = \frac{\partial}{\partial \text{pH}} \left( \frac{\partial H}{\partial T} \right) = \frac{\partial C_p}{\partial \text{pH}}. \quad (18)$$

With regard to the heat capacity measured by DSC, to our knowledge there has been no report which clearly described the pH dependence of native heat capacity. However, the deprotonation in the acidic region by increasing pH is likely to decrease the heat capacity of the native state by increasing the hydrophilic hydration, corresponding to the negative pH dependence of the heat capacity observed in this study.

In summary, we have established several new methods for precisely and reproducibly determining the enthalpy of a protein molecule as a function of pH under a fixed temperature using IATC data and pH measurement. Using the enthalpy function and the pH transition of the three-dimensional structure of the protein, the thermodynamic parameters accompanying the transition, such as enthalpy change, midpoint pH, and proton binding-number difference, are estimated by assuming a thermodynamic model for the transition. The acid-denaturation enthalpy of bovine ribonuclease A determined by this method agreed well with the enthalpy change calculated by the traditional, highly sensitive DSC, and the thermodynamic parameters were found to well explain the acid-transition of the three-dimensional structure monitored by far UV CD spectrum. These results clearly show the accuracy of the thermodynamic functions obtained by this new method. The van't Hoff enthalpy of the transition can be derived from the temperature dependence of the midpoint pH and the proton binding-number difference, and can be used to check the validity of the assumed thermodynamic model necessary to determine the thermodynamic parameters from the enthalpy function. The van't Hoff enthalpy of bovine ribonuclease A at  $40^\circ \text{C}$ , pH 2.8 agreed with the calorimetric enthalpy directly observed by acid-titration calorimetry under the same solution conditions. The

agreement between the two enthalpies indicated that there was no stable intermediate state during the pH transition of this protein, and also suggested that this method could accurately the van't Hoff enthalpy. The enthalpy function of ribonuclease A indicated that the magnitude of the pH dependence of enthalpy change at the constant temperature,  $[\partial\Delta H/\partial\text{pH}]_T$ , was less than  $3 \text{ kJ pH}^{-1} \text{ mol}^{-1}$  at  $40^\circ\text{C}$ , which makes for a 3% or smaller correction for the evaluation of the heat capacity change of the transition using the slope of the  $\Delta H(T_m)$  vs.  $T_m$  plot.

Since protons naturally ligate to protein molecules, the new methods presented here are expected to be applicable to the thermodynamic evaluation of the stability of many kinds of proteins, without requirement of increasing temperature and without buffering reagent or denaturant. In addition, this method could be applied to thermodynamically evaluate various kinds of biological phenomena induced by proton binding and/or pH change, such as the acid-activation of zymogens or the pH-induced intermediate state of protein folding.

## References

- [1] N.N. Khechinashvili, P.L. Privalov, E.I. Tiktopulo, Calorimetric investigation of lysozyme thermal denaturation, *FEBS Lett.* 30 (1973) 57–60.
- [2] P.L. Privalov, N.N.A. Khechinashvili, thermodynamic approach to the problem of stabilization of globular protein structure: a calorimetric study, *J. Mol. Biol.* 86 (1974) 665–684.
- [3] W. Pfeil, P.L. Privalov, Thermodynamic investigations of proteins. I. Standard functions for proteins with lysozyme as an example, *Biophys. Chem.* 4 (1976) 23–32.
- [4] W. Pfeil, P.L. Privalov, Thermodynamic investigations of proteins. II. Calorimetric study of lysozyme denaturation by guanidine hydrochloride, *Biophys. Chem.* 4 (1976) 33–40.
- [5] P.L. Privalov, Stability of proteins: small globular proteins, *Adv. Protein. Chem.* 33 (1979) 167–241.
- [6] P.L. Privalov, Stability of proteins. Proteins which do not present a single cooperative system, *Adv. Protein. Chem.* 35 (1982) 1–104.
- [7] P.L. Privalov, Y.U.V. Griko, S.Y.U. Venyaminov, V.P. Kutysenko, Cold denaturation of myoglobin, *J. Mol. Biol.* 190 (1986) 487–498.
- [8] R. Kuroki, K. Inaka, Y. Taniyama, S. Kidokoro, M. Matsushima, M. Kikuchi, et al., Enthalpic destabilization of a mutant human lysozyme lacking a disulfide bridge between cysteine-77 and cysteine-95, *Biochemistry* 31 (1992) 8323–8328.
- [9] G.I. Makhatadze, P.L. Privalov, Contribution of hydration to protein folding thermodynamics. I. The enthalpy of hydration, *J. Mol. Biol.* 232 (1993) 639–659.
- [10] P.L. Privalov, G.I. Makhatadze, Contribution of hydration to protein folding thermodynamics. II. The entropy and Gibbs energy of hydration, *J. Mol. Biol.* 232 (1993) 660–679.
- [11] G.I. Makhatadze, P.L. Privalov, Energetics of protein structure, *Adv. Protein. Chem.* 47 (1995) 307–425.
- [12] J. Funahashi, K. Takano, Y. Yamagata, K. Yutani, Role of surface hydrophobic residues in the conformational stability of human lysozyme at three different positions, *Biochemistry* 39 (2000) 14448–14456.
- [13] K. Takano, Y. Yamagata, K. Yutani, Contribution of polar groups in the interior of a protein to the conformational stability, *Biochemistry* 40 (2001) 4853–4858.
- [14] E. Freire, R.L. Biltonen, Statistical mechanical deconvolution of thermal transitions in macromolecules. I. Theory and application to homogeneous systems, *Biopolymers* 17 (1978) 463–479.
- [15] S. Kidokoro, A. Wada, Determination of thermodynamic functions from scanning calorimetry data, *Biopolymers* 26 (1987) 213–229.
- [16] S. Kidokoro, H. Uedaira, A. Wada, Determination of thermodynamic functions from scanning calorimetry data II, *Biopolymers* 27 (1988) 271–297.
- [17] P.L. Privalov, G.I. Makhatadze, Heat capacity of proteins. II. Partial molar heat capacity of the unfolded polypeptide chain of proteins: protein unfolding effects, *J. Mol. Biol.* 213 (1990) 385–391.
- [18] G.I. Makhatadze, P.L. Privalov, Heat capacity of proteins. I. Partial molar heat capacity of individual amino acid residues in aqueous solution: hydration effect, *J. Mol. Biol.* 213 (1990) 375–384.
- [19] V.V. Loladze, D.N. Ermolenko, G.I. Makhatadze, Heat capacity changes upon burial of polar and non-polar groups in proteins, *Protein. Sci.* 10 (2001) 1343–1352.
- [20] C.N. Pace, G.R. Grimsley, S.T. Thomas, G.I. Makhatadze, Heat capacity change for ribonuclease A folding, *Protein. Sci.* 8 (1999) 1500–1504.
- [21] S. Kidokoro, Y. Miki, A. Wada, Physical and biological stability of globular proteins, in: M. Hatano (Ed.), *Protein Structural Analysis, Folding and Design*, JSSP and Elsevier, Tokyo, 1990, pp. 75–91.
- [22] W. Pfeil, P.L. Privalov, Thermodynamic investigations of proteins. I. Standard functions for proteins with lysozyme as an example, *Biophys. Chem.* 4 (1976) 23–32.
- [23] M. Jamin, M. Antalík, S.N. Loh, D.W. Bolen, R.L. Baldwin, The unfolding enthalpy of the pH 4 molten globule of apomyoglobin measured by isothermal titration calorimetry, *Protein. Sci.* 9 (2000) 1340–1346.
- [24] A. Tamura, J.M. Sturtevant, A thermodynamic study of mutant forms of *Streptomyces subtilisin* inhibitor. I.

- Hydrophobic replacements at the position of Met103, *J. Mol. Biol.* 249 (1995) 625–635.
- [25] A. Tamura, S. Kojima, K. Miura, J.M. Sturtevant, A thermodynamic study of mutant forms of *Streptomyces subtilisin* inhibitor. II. Replacements at the interface of dimer formation, *Val13*, *J. Mol. Biol.* 249 (1995) 636–645.
- [26] S.A. Petrosian, G.I. Makhatadze, Contribution of proton linkage to the thermodynamic stability of the major cold-shock protein of *Escherichia coli* CspA, *Protein Sci.* 9 (2000) 387–394.
- [27] V. Bhakuni, D. Xie, E. Freire, Thermodynamic identification of stable folding intermediates in the B-subunit of cholera toxin, *Biochemistry* 30 (1991) 5055–5060.
- [28] D. Hamada, S. Kidokoro, H. Fukada, K. Takahashi, Y. Goto, Salt-induced formation of the molten globule state of cytochrome *c* studied by isothermal titration calorimetry, *Proc. Natl. Acad. Sci. USA* 91 (1994) 10325–10329.
- [29] G.L. Bertrand, F.J. Millero, C. Wu, L.G. Helper, Thermochemical investigations of the water–ethanol and water–methanol solvent systems. I. Heats of mixing, heats of solution, and heats of ionization of water, *J. Phys. Chem.* 70 (1966) 699–705.
- [30] T. Nakagawa, T. Oyanagi, Program system SALS for non-linear least-squares fitting in experimental sciences, in: K. Matusuta (Ed.), *Recent Developments in Statistical Inference and Data Analysis*, North Holland Publishing Company, 1980, pp. 221–225.
- [31] D.J. Quirk, C. Park, J.E. Thompson, R.T. Raines, His–Asp catalytic dyad of ribonuclease A: conformational stability of the wild-type, D121 N, D121A, and H119A enzymes, *Biochemistry* 37 (1998) 17958–17964.
- [32] M.T. Cederholm, J.A. Stuckey, M.S. Doscher, L. Lee, Histidine  $pK_a$  shifts accompanying the inactivating Asp121→Asn substitution in a semisynthetic bovine pancreatic ribonuclease, *Proc. Natl. Acad. Sci. USA* 88 (1991) 8116–8120.
- [33] D.J. Quirk, R.T. Raines, His–Asp catalytic dyad of ribonuclease A: histidine  $pK_a$  values in the wild-type, D121 N, and D121A enzymes, *Biophys. J.* 76 (1999) 1571–1579.
- [34] R.M. Izatt, J.J. Christensen, *Handbook of Biochemistry and Molecular Biology, Physical and Chemical Data*, CRC Press, Cleveland, 1976.
- [35] H. Fukada, K. Takahashi, Enthalpy and heat capacity changes for the proton dissociation of various buffer components in 0.1 M potassium chloride, *Proteins* 33 (1998) 159–166.